ACS APPLIED MATERIALS & INTERFACES

Research Article

www.acsami.org

Engineering a Highly Hydrophilic PVDF Membrane via Binding TiO_2 Nanoparticles and a PVA Layer onto a Membrane Surface

Aiwen Qin, Xiang Li, Xinzhen Zhao, Dapeng Liu, and Chunju He*

The State Key Laboratory for Modification of Chemical Fibers and Polymer Materials, College of Materials Science and Engineering Donghua University, Shanghai, 201620, People's Republic of China

ABSTRACT: A highly hydrophilic PVDF membrane was fabricated through chemically binding TiO_2 nanoparticles and a poly(vinyl alcohol) (PVA) layer onto a membrane surface simultaneously. The chemical composition of the modified membrane surface was determined by X-ray photoelectron spectroscopy, and the binding performance of TiO_2 nanoparticles and the PVA layer was investigated by a rinsing test. The results indicated that the TiO_2 nanoparticles were uniformly and strongly tailored onto the membrane surface, while the PVA layer was firmly attached onto the surface of TiO_2 nanoparticles and the membrane by adsorption-cross-linking. The possible mechanisms during the modification process and filtration performance, i.e., water permeability and bovine serum albumin (BSA) rejection, were investigated as well. Furthermore, antifouling property was discussed through multicycles of BSA solution filtration tests, where the flux recovery ratio was significantly increased from 20.0% for pristine PVDF membrane to 80.5% for PVDF/TiO_2/PVA-modified membrane. This remarkable promotion is mainly ascribed to the improvement of surface hydrophilicity, where the water contact angle of the membrane surface was decreased from 84° for pristine membrane to 24° for PVDF/TiO_2/PVA membrane. This study presents a novel and varied strategy for immobilization of nanoparticles and PVA layer on substrate surface, which could be easily adapted for a variety of materials for surface modification.

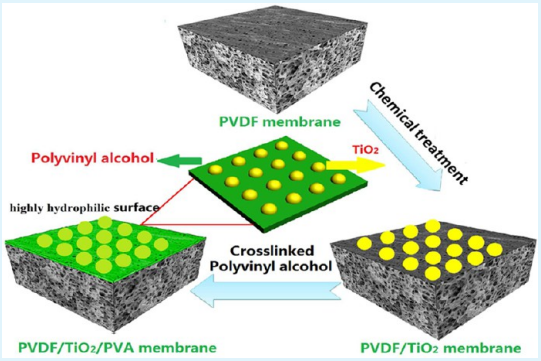

KEYWORDS: *polyvinylidene fluoride, surface modification, TiO_2, poly(vinyl alcohol), antifouling property*

INTRODUCTION

Polyvinylidene fluoride (PVDF) membrane has been extensively used in microfiltration and ultrafiltration processes for industrial application because of its excellent mechanical properties, thermal stability, and chemical resistance.[1−3] However, the strong hydrophobic nature of pure PVDF membrane always leads to low water permeability and easy fouling while treating an aqueous solution containing some natural organic and colloidal matters which are prone to deposition and absorption onto the membrane surface.[4−11] This inevitably depresses the lifetime of the membrane and subsequently leads to more operation cost of replacement.[12−16] As a simple modification method, the incorporation of nanomaterials to impart the antifouling property of the membrane has attracted significant interest in recent years due to the facile processing, and commonly used nanomaterials mainly include titanium dioxide,[17−19] silicon dioxide,[20,21] aluminum oxide,[22] and carbon nanotubes.[23,24]

Some literature reports about blending titanium dioxide (TiO_2) nanoparticles into PVDF membrane have shown the effectiveness to improve membrane hydrophilicity and antifouling ability.[25,26] Unfortunately, exhibition of the improvement in membrane hydrophilicity and resistance to membrane fouling is limited due to the poor dispersibility and entirely enfolded by polymer matrix, which significantly decreases the modification efficiency. Tailoring TiO_2 nanoparticles on the membrane surface through self-assembly or a chemical bonding process has been proven to be an effective strategy to improve the hydrophilicity and antifouling property of PVDF membranes compared with the nanoparticles blending strategy,[5,12,13,17,27] since all TiO_2 nanoparticles are entirely exposed to the environment rather than entrapped in membrane matrix. Furthermore, it presents a uniform dispersion of TiO_2 nanoparticles on the membrane surface, which can effectively decline the blocking probability of membrane surface pores. However, these approaches seem to be not efficient under a relatively high TiO_2 concentration to modify the PVDF membrane due to the weak binding force between the membrane surface and the nanoparticles.[28−31] Nevertheless, the quantity and density of TiO_2 nanoparticles on the membrane surface directly decide the efficiency of surface modification, and the firm binding of TiO_2 nanoparticles can ensure the long-lasting hydrophilicity and reduce water permeation resistance. Therefore, it is necessary to develop an effective and facile strategy to uniformly disperse TiO_2 on the membrane surface with the strong binding force for improving membrane performance.

Received: October 11, 2014
Accepted: March 25, 2015
Published: March 25, 2015

DOI: 10.1021/acsami.5b00978
ACS Appl. Mater. Interfaces 2015, 7, 8427−8436

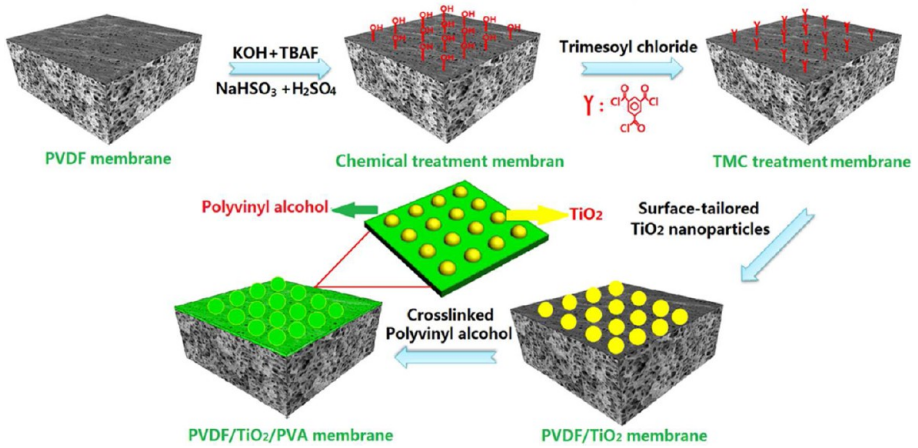

Figure 1. Schematic illustration of the PVDF membrane surface modification.

Recently, poly(vinyl alcohol) (PVA) has been widely used as a selective and functionalized skin layer for a thin film composite membrane via adsorption-cross-linking with regard to its high hydrophilicity, excellent mechanical strength, and chemical resistance,[32−35] and many literature reports have confirmed that the PVA-modified surface exhibited a remarkable enhancement of hydrophilicity as well as antifouling property.[32,36,37] Du et al.[38] modified a PVDF flat sheet membrane by surface coating PVA, which exhibited a slower fouling rate compared to pristine membrane during natural water filtration. Nevertheless, the interaction between a coated PVA layer and the membrane surface was relatively weak, which inevitably led to the peeling or delamination of the hydrophilic coating from the membrane surface during long-term operation. Actually, a recent study by Puspitasari et al.[39] has revealed that the coated substance on the PVDF membrane surface could be removed during the membrane cleaning process.

This present paper demonstrates a facile surface modification approach for hydrophobic PVDF membrane. Hydroxyl groups were introduced onto the prepared membrane surface through a chemical treatment process, which would form a strong chemical bond for binding TiO_2 nanoparticles on the membrane surface using trimesoyl chloride as a bridge. Afterward, the separate TiO_2 nanoparticles were further bonded together by a cross-linked PVA thin layer, which effectively inhibited the shedding of single nanoparticles from the membrane surface. Meanwhile, the fixed TiO_2 nanoparticles provided some anchor sites for the PVA layer as well, which effectively inhibited the peeling or delamination of the PVA thin layer from the membrane surface and overcame the limitation caused by the surface coating method. The hydrophilicity of the resulting membrane presented a remarkable improvement, where the water contact angle is decreased from 84° for pristine membrane to 24° for PVDF/TiO_2/PVA membrane. Furthermore, the hydrophilicity kept a significant stability and durability in the long-term rinsing process. To the best of our knowledge, there is no such a strategy reported to fix TiO_2 nanoparticles and PVA layer on the surface of a PVDF membrane simultaneously with tight binding for performance enhancement.

EXPERIMENTAL SECTION

Materials. PVDF powder (Kynar) was supplied by Arkema Inc. Poly(vinyl alcohol) (PVA, 1799), *N*,*N*-dimethylacetamide, polyvinylpyrrolidone (PVP, K30), glutaraldehyde, γ-butyrolactone, anhydrous ethanol, sulfuric acid, trimesoyl chloride (TMC, 98%), potassium hydroxide (KOH), sodium bisulfite ($NaHSO_3$), and hexane were obtained from Shanghai Chemical Reagents Medicine Group Co., Ltd. Tetrabutylammonium fluoride (TBAF, 98%), titanium dioxide powder (anatase, <50 nm, 99.7%), and bovine serum albumin (BSA, M_n = 67 000) were purchased from Sigma-Aldrich. All chemicals and materials were used without further purification.

Preparation of PVDF Membrane. The casting solution of the pristine PVDF membrane was prepared as follows: 18 g of PVDF and 2 g of PVP were dissolved in 70 g of a *N*,*N*-dimethylacetamide/γ-butyrolactone (1:2, volume ratio) mixed solution at 100 °C under mechanical stirring for 6 h. Afterward, the solution was degassed for 12 h and cast on a glass plate with a steel knife and immediately immersed into a deionized water bath with a temperature of 25 ± 1 °C. The membrane precursor was obtained within a few seconds through phase inversion. The nascent membranes were washed until the residual solvent was entirely removed and then placed in a deionized water bath for the test and characterization.

Surface Modification of PVDF Membranes. Prior to surface modification of the PVDF membrane, the wet membranes were successively immersed in ethanol and hexane for 30 min and then dried in air at room temperature for modification. The schematic illustration of the surface modification of the membranes is presented in Figure 1, and the detailed procedure is depicted as follows: (1) pristine PVDF membranes were dipped into 200 mL of KOH aqueous solution (1 mol/L) for 30 min at 25 °C with 0.5 g of TBAF as phase transfer catalyst and then directly immersed in $NaHSO_3$ aqueous solution (1 mol/L) for 30 min with 0.1 g of H_2SO_4 as catalyst at 25 °C; (2) the $NaHSO_3$ pretreated membranes were directly immersed into 0.5 wt % trimesoyl chloride hexane solution for 2 min at 25 °C; (3) the membranes were taken out from the trimesoyl chloride and directly immersed in the previously prepared TiO_2 suspension (0.01, 0.04, and 0.08 wt %, ultrasonic dispersion for 30 min) for 10 min, and then the membranes were taken out and washed with deionized water; afterward, the TiO_2 modified membranes were obtained and labeled as PVDF/TiO_2-0.01, PVDF/TiO_2-0.04, and PVDF/TiO_2-0.08, respectively; (4) the TiO_2-modified membranes were dipped into 1 wt % PVA solution for 4 min with glutaraldehyde and H_2SO_4 used as cross-linker and catalyst, respectively; then the membranes were taken out and heated in a vacuum oven for 10 min at 60 °C to promote the cross-linking reaction of PVA. Afterward, the resulting membranes were then thoroughly rinsed with distilled water and soaked in distilled water on a shaker for 12 h to remove traces of unreacted glutaraldehyde and PVA, and then stored in distilled water before use.

Characterization of the Physical and Chemical Properties of Membranes. The wet membranes were successively immersed in ethanol and hexane for 30 min and subsequently dried in air for the following testing. The surface morphology of the membranes was examined by a field emission scanning electron microscope (FESEM,

DOI: 10.1021/acsami.5b00978
ACS Appl. Mater. Interfaces 2015, 7, 8427−8436

Hitachi, S-4800, Japan). Membrane surface chemical composition was tested using X-ray photoelectron spectroscopy (XPS, Shimadzu AXIS Ultra DLD, Japan) with a resolution of 0.68 eV/(C 1s); the takeoff angle of photoelectron radiation was set at 90°. The membrane surface roughness was investigated by atomic force microscopy (AFM, Bioscope Catalyst, USA) with tapping mode at room temperature in air. In addition, Fourier transform infrared (FTIR) absorption spectra of the membranes were measured with a Nicolet 8700 (Thermo Electron Corp, USA) in the range of 4000−400 cm^{-1} with an attenuated total reflection (ATR) accessory. The hydrophilicity of the membranes was evaluated by a contact angle measuring instrument (OCA40micro, Germany). The measurement was conducted by dropping 2 μL of water on the surface of the membrane. The initial contact angle of the sample was adopted, and at least five positions for each sample were tested and then averaged.

Filtration Experiments. The water permeability and BSA rejection of membrane were conducted on a dead-end filtration system at a constant transmembrane pressure of 0.1 MPa and 25 ± 2 °C. The effective membrane area was 4.56 cm^2, and 0.5 g/L BSA aqueous solution was applied to the rejection experiment. Each membrane was initially prepressured at 0.1 MPa with deionized water for 40 min before testing. The BSA concentration of the permeation and feed solution was determined by an UV−vis spectrophotometer (UV-1800, Shimadzu) at a wavelength of 280 nm. The permeation fluxes (J_w) and BSA rejection (R) were calculated by the following equations, respectively

$$J_w = \frac{V}{A \cdot \Delta t} \tag{1}$$

where V (L) is the volume of permeated water, A (m^2) is the membrane effective area, and Δt (h) is the permeation time.

$$R = \left(1 - \frac{C_P}{C_F}\right) \times 100\% \tag{2}$$

where C_P and C_F are the BSA concentration of permeation and feed solution, respectively. C_F was maintained at 0.5 g/L, while C_P was sampled in permeation solution after 30 min BSA ultrafiltration.

Antifouling Property Evaluation. To evaluate the fouling resistance of various membranes, the membrane was subjected to a protein solution permeation test using BSA as the model protein. Each membrane was prepressured at 0.1 MPa with deionized water−water for 40 min until the flux reached a stable value and recorded the water flux J_1 ($L \cdot m^{-2} \cdot h^{-1}$). Subsequently, BSA solution replaced the deionized water at a transmembrane pressure of 0.1 MPa for 30 min, and then BSA solution flux was recorded J_p ($L \cdot m^{-2} \cdot h^{-1}$). Afterward, the membranes were washed with deionized water for 30 min in the direction of filtration, and then the water flux of cleaned membranes J_2 ($L \cdot m^{-2} \cdot h^{-1}$) was recorded, indicating the end of one filtration cycle.

In order to examine the antifouling property of these membranes in details, the flux recovery ratio (F_{rr}) and total fouling ratio (R_t) were defined and calculated by following equations

$$F_{rr} = \frac{J_2}{J_1} \times 100\% \tag{3}$$

$$R_t = \left(1 - \frac{J_p}{J_1}\right) \times 100\% \tag{4}$$

Here, R_t is the degree of total flux loss caused by total fouling, and it is the sum of the reversible fouling ratio (R_r) and irreversible fouling ratio (R_{ir}). R_r denotes the fouling caused by concentration polarization, and R_{ir} describes the fouling caused by adsorption or deposition of protein molecules on the membrane surface, which can be calculated by the following equations

$$R_r = \frac{J_2 - J_p}{J_1} \times 100\% \tag{5}$$

$$R_{ir} = \frac{J_1 - J_2}{J_1} \times 100\% \tag{6}$$

Characterization of TiO_2 Binding Performance. The binding performance of TiO_2 nanoparticles on the membrane surface was investigated by a flexible rinsing experiment, which was carried out in a 2 L beaker. The modified membranes were initially fixed on the glass wall of the beaker by scotch tape with the membrane bottom surface attached to the glass; then about 1.5 L of distilled water was filled in the beaker and magnetically stirred at 1000 r/min for 2 h. Finally, the surface morphology and water contact angle of modified membranes before and after rinsing were characterized and measured.

RESULTS AND DISCUSSION

Characterization of Pristine and Modified Membranes. The pristine PVDF membrane was premodified in alkaline aqueous solution and TMC hexane media, respectively, for forming reactive groups (−COCl) to chemical bonding TiO_2 nanoparticles onto membrane surface. Afterward, the TiO_2 nanoparticles of the membrane surface were further fixed by followed adsorption-cross-linking of PVA. Figure 1 illustrates the whole modification process in detail. In order to demonstrate the modification effect, the physical and chemical properties of the pristine and modified membranes were investigated below.

The PVDF membrane chemical treatment procedure mainly involved two steps: dehydrofluorination and nucleophilic addition. The pristine membrane was treated by KOH aqueous solution to facilitate the formation of unsaturated double bonds, which were used for nucleophilic addition reaction to introduce a hydroxyl group on the polymer chains.[40,41] It can be observed that the pristine PVDF membrane is white, while a light brown color is shown after chemical treatment. This result indicates the successful hydroxy modification of the membrane surface, which is further confirmed by the ATR-FTIR spectra for qualitative analysis as shown in Figure 2. The peak of 1400 cm^{-1} is associated with the deformation vibration of $-CH_2$, and the vibration bonds at 1275, 1178, and 875 cm^{-1} are considered as the characteristic peaks of PVDF.[42,43] A new broad peak between 3600 and 3100 cm^{-1} appears for the chemical treatment membrane (Figure 2b) compared with the pristine

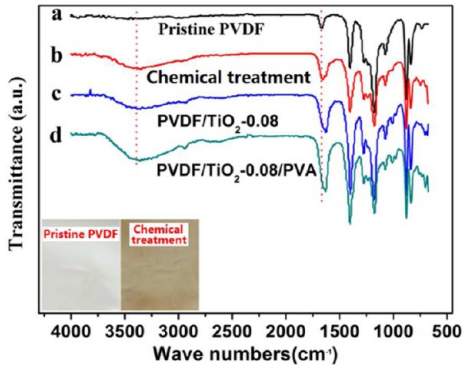

Figure 2. ATR-FTIR spectra of various membranes: (a) pristine PVDF membrane; (b) chemical treatment membrane (pristine PVDF membrane was treated by KOH and $NaHSO_3$ successively); (c) PVDF/TiO_2-0.08 membrane (chemical treatment membrane was pretreated by TMC hexane media and then bonding TiO_2 nanoparticles); (d) PVDF/TiO_2-0.08/PVA membrane (adsorption-cross-linking of PVA layer on PVDF/TiO_2 membrane surface). (Inset) Color for pristine and chemical treatment membrane.

DOI: 10.1021/acsami.5b00978
ACS Appl. Mater. Interfaces 2015, 7, 8427−8436

membrane (Figure 2a), which is ascribed to O−H stretching vibration.[44] PVA typically enhances absorbency intensity at 3400 and 1100 cm^{-1} for its −OH group and at 2950 and 1409 cm^{-1} for its $-CH_2$ groups.[34] Compared with the pristine membrane (Figure 2a), the PVDF/TiO_2-0.08/PVA-modified membrane (Figure 2d) has intense and wider peaks at 3400 cm^{-1} due to the hydroxyl group from PVA and TiO_2 and at 1638 cm^{-1} from adsorbed water.[36] Additionally, the peak at 1670 cm^{-1} is mainly attributed to a C═O stretching vibration resulting from the residual PVP in the final membrane,[45] which will be further proved through XPS analysis.

Figure 3 shows XPS wide spectra for various membranes: there are two peaks of O (1s) and N (1s) in pristine membrane,

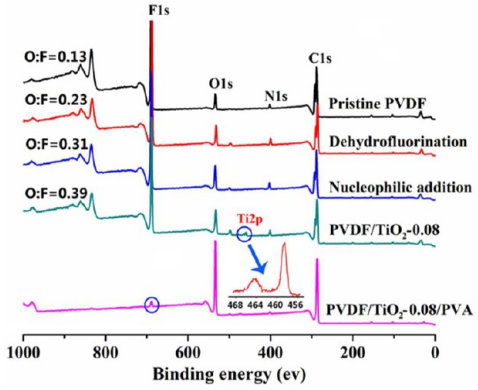

Figure 3. XPS wide spectra for pristine PVDF membrane, dehydrofluorination membrane, nucleophilic addition membrane, PVDF/TiO_2-0.08 membrane, and PVDF/TiO_2-0.08/PVA membrane, and atom ratio (O: F) of various membranes.

which is consistent with the above result of the ATR-FTIR test and further proves the remnant of PVP in the final membranes. Furthermore, the atom ratio (O:F) is increased from 0.13 for pristine membrane to 0.23 for dehydrofluorination membrane and then gradually increases to 0.31 for nucleophilic addition membrane, which implies completion of the oxidation−reduction reaction and introduction of a hydroxyl group on the membrane surface. A new peak of Ti (2p) appears except for the peaks of F (1s), O (1s), N (1s), and C (1s) as for the PVDF/TiO_2-0.08 membrane, and it can be clearly seen from the partial enlarged view that the peak of Ti (2p) is constituted by two peaks located at 464.1 and 458.2 eV, which correspond to Ti ($2p_{1/2}$) and Ti ($2p_{3/2}$), respectively, indicating a normal state of Ti^{4+} in TiO_2, which confirms the instant binding of TiO_2 particles onto the TMC-pretreatment membrane. Additionally, the continuous increase of the atom ratio (O:F) can also confirm the bonding of TiO_2 on the membrane surface. However, the XPS wide spectra of PVDF/TiO_2-0.08/PVA displays a dramatic change compared with that of other membranes. The intensity of peaks of F (1s) and N (1s) is greatly weakened, and the peak of Ti (2p) almost disappears, whereas the intensity of O (1s) and C (1s) is markedly increased, which verifies the fact that the PVA layer can be firmly attached onto the surface of TiO_2 nanoparticles and membranes by adsorption-cross-linking.

Figure 4 illustrates the possible mechanism of the PVA layer and TiO_2 nanoparticles binding process. The chemical treatment membranes were first immersed into TMC hexane medium to introduce chloride groups, which could react with the hydroxyl group of TiO_2, and strong coordination bonds could be formed between membranes and nanoparticles. This in situ attraction of TiO_2 assists the homogeneous distribution and tight binding of TiO_2 nanoparticles on the PVDF

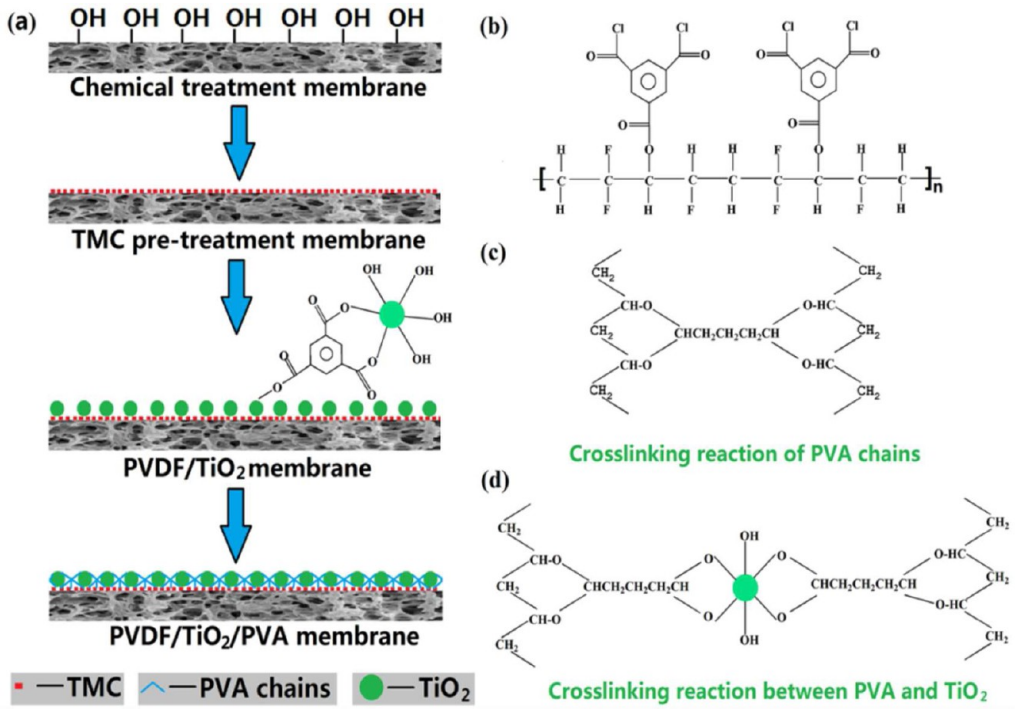

Figure 4. Possible mechanism of PVA layer and TiO_2 nanoparticles binding process: (a) binding process of PVA layer and TiO_2 nanoparticles; (b) reaction between chemical treatment membrane and TMC; (c) cross-linking reaction of PVA chains; (d) cross-linking reaction between PVA and TiO_2 nanoparticles.

DOI: 10.1021/acsami.5b00978
ACS Appl. Mater. Interfaces 2015, 7, 8427−8436

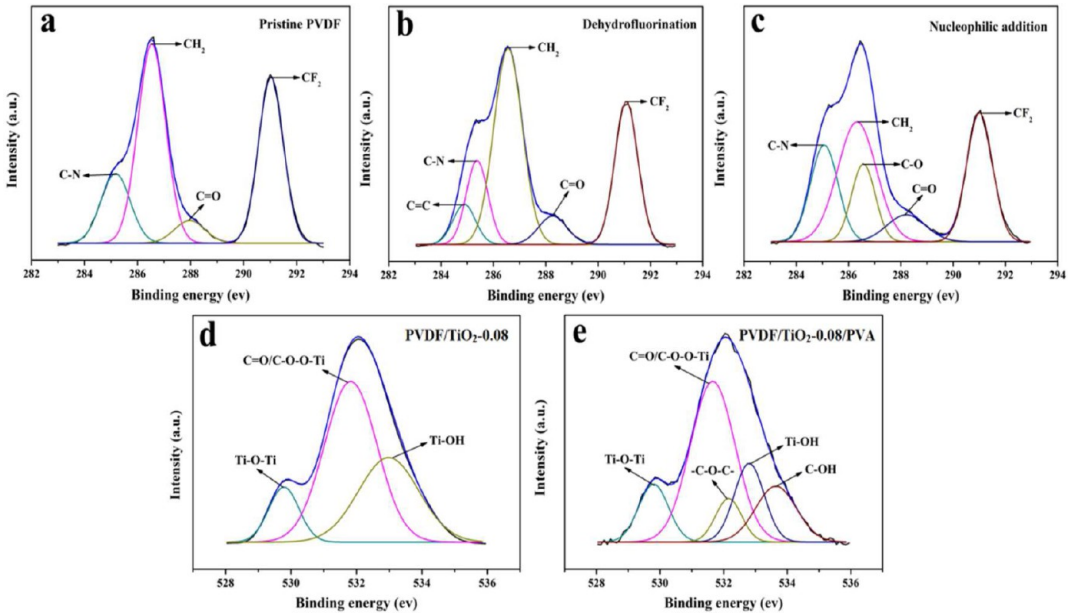

Figure 5. C (1s) core level spectra resolved results of pristine PVDF membrane (a), dehydrofluorination membrane (b), and nucleophilic addition membrane (c); O (1s) core level spectra resolved results of PVDF/TiO_2-0.08 membrane (d) and PVDF/TiO_2-0.08/PVA membrane (e).

membrane surface. Subsequently, the modified PVDF membrane with TiO_2 nanoparticles was immersed into PVA aqueous solution and a cross-linking reaction conducted between the PVA molecular chains. The formed hydrophilic PVA layer will further contribute to binding the nanoparticles of the membrane surface for potential performance enhancement. In addition, the cross-linking reaction could be carried out between PVA and nanoparticles as well, which will inhibit the peeling or delamination of the hydrophilic PVA layer from the membrane surface. This result is further confirmed by the C (1s) and O (1s) core level spectra resolved results for various membranes as shown in Figure 5. The C (1s) peak of pristine PVDF membrane can be resolved into four peaks corresponding to CF_2 (291.1 eV) and CH_2 (286.6 eV) assigned to PVDF[46] and C−N (285.2 eV) and C═O (288.1 eV) assigned to PVP according to previous reports.[47−49] A new peak C═C (284.9 eV) for the dehydrofluorination membrane appears compared with the pristine membrane and is then replaced by a C−O (286.3 eV) peak with further nucleophilic addition reaction.[46] This result is consistent with the above results of ATR-FTIR, indicating successful introduction of a hydroxyl group on polymer chains. As shown in Figure 5d, three peaks located at 529.8, 531.8, and 532.9 eV can be obtained, which correspond to Ti−O−Ti, C═O/C−O−O−Ti, and Ti−OH species, respectively.[50,51] Additionally, two other new peaks located at 532.1 (−C−O−C) and 533.6 eV (C−OH) are observed for the PVDF/TiO_2-0.08/PVA membrane,[46,47] which is mainly induced by the adsorption-cross-linking of PVA on the membrane surface. These results indicate that the surface composition of membranes is successfully modified by TiO_2 nanoparticles and PVA, which will contribute to the enhancement of hydrophilicity of membrane surface.

The surface morphology of pristine and modified membranes in Figure 6 shows that the nanoparticles are uniformly dispersed on the membrane surface; the quantity and density of immobilized TiO_2 nanoparticles is gradually increased with increasing concentration of nanoparticles in suspension. When the TiO_2 suspension contacts with TMC premodified

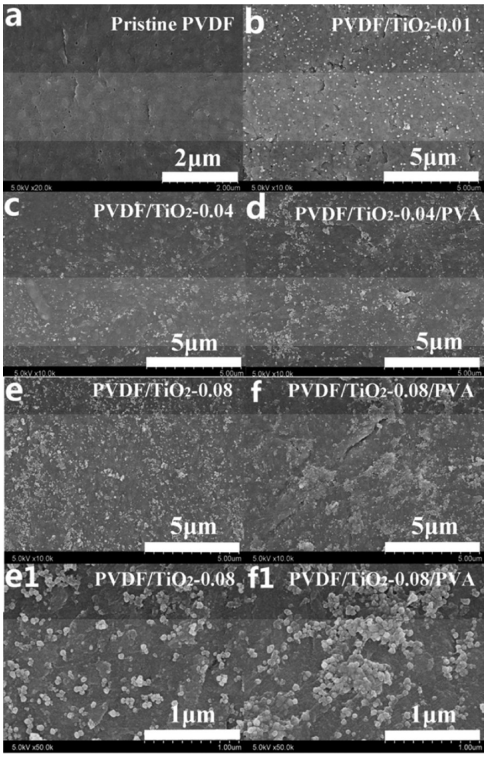

Figure 6. Surface morphology of various membranes: (a) pristine PVDF membrane; (b) PVDF/TiO_2-0.01 membrane; (c) PVDF/TiO_2-0.04 membrane; (d) PVDF/TiO_2-0.04/PVA membrane; (e) PVDF/TiO_2-0.08 membrane; (f) PVDF/TiO_2-0.08/PVA membrane; (e1 and f1) partial enlarged views of e and f.

membrane surface, the higher concentration of TiO_2 provides more chance for nanoparticles to attach to acid chloride groups and more nanoparticles are covered on the membrane surface. Moreover, it can be obviously found from the partial enlarged view in Figure 6f1 that the formed hydrophilic PVA layer is effectively adhered to the surface of nanoparticles and

DOI: 10.1021/acsami.5b00978
ACS Appl. Mater. Interfaces 2015, 7, 8427−8436

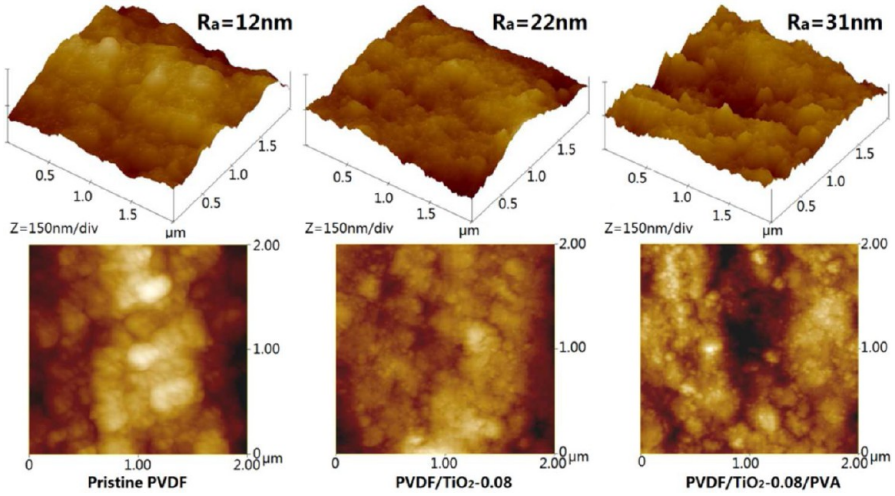

Figure 7. AFM images of pristine PVDF membrane, PVDF/TiO_2-0.08 membrane, and PVDF/TiO_2-0.08/PVA membrane; Ra, mean surface roughness.

membrane, which will significantly contribute to the stabilization of nanoparticles on the membrane surface.

The three-dimensional AFM pictures of various membranes presented in Figure 7 show that the smooth surface of the pristine membrane becomes rough after immobilization of TiO_2, which is mainly attributed to the chemical bonding between nanoparticles and the membrane surface. After the following adsorption-cross-linking of PVA, some obvious peaks and valleys are observed and the mean surface roughness is continuously increased from 22 to 31 nm due to the packing of PVA on the nanoparticles surface. In addition, some PVA fragments resulting from cross-linking reaction among the PVA molecular chains may also contribute to the roughness of the membrane surface.

The water contact angle is employed to evaluate the relative surface hydrophilicity of different membranes. In general, the smaller contact angle indicates the better hydrophilicity of membranes. As shown in Figure 8, the pristine PVDF membrane possesses the highest contact angle of 84°, corresponding to the lowest surface hydrophilicity. The hydrophilicity of the chemical treatment membrane is significantly improved compared with the pristine membrane since amounts of hydroxyl groups are formed on the membrane surface. The water contact angle of the TiO_2-modified membrane is decreased from 52° to 40° with increasing of TiO_2 content. This result should be ascribed to the quantity and density of embedded TiO_2 nanoparticles on the membrane surface, which leads to improvement of the surface hydrophilicity. After the adsorption-cross-linking of PVA on the membrane surface, the water contact angle of the final membrane is abruptly decreased to 24° resulting from the combined action of the hydrophilic TiO_2 nanoparticles and the PVA layer, implying the impressive enhancement in hydrophilicity.

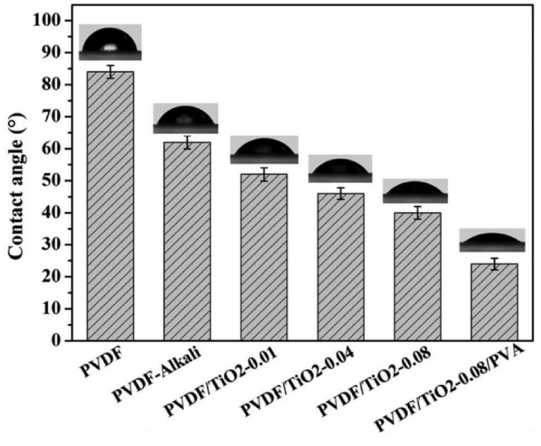

Figure 8. Water contact angle of the pristine and modified membranes.

Water Permeability and BSA Rejection. Solute separation and solvent permeation, as two fundamental and essential properties of a membrane, are evaluated by BSA rejection and water permeability measurement, respectively. As shown in Figure 9, pure water flux of the chemical treatment membrane exhibits a significant increase compared with that of pristine membrane, while the BSA rejection displays a contrary tendency. This is mainly due to the etching effect by alkali solution in the chemical treatment process.[52] In addition, pure water flux presents a decline tendency with increasing TiO_2 concentration on the membrane surface; this result is mainly due to formation of the TiO_2 layer increasing the water permeation resistance. After the following adsorption-cross-

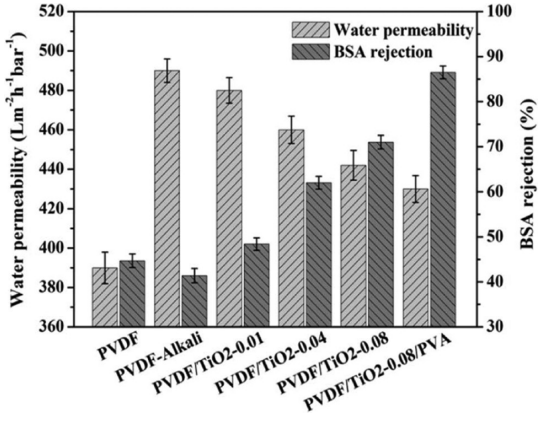

Figure 9. Water permeability and BSA rejection of various membranes.

DOI: 10.1021/acsami.5b00978
ACS Appl. Mater. Interfaces 2015, 7, 8427−8436

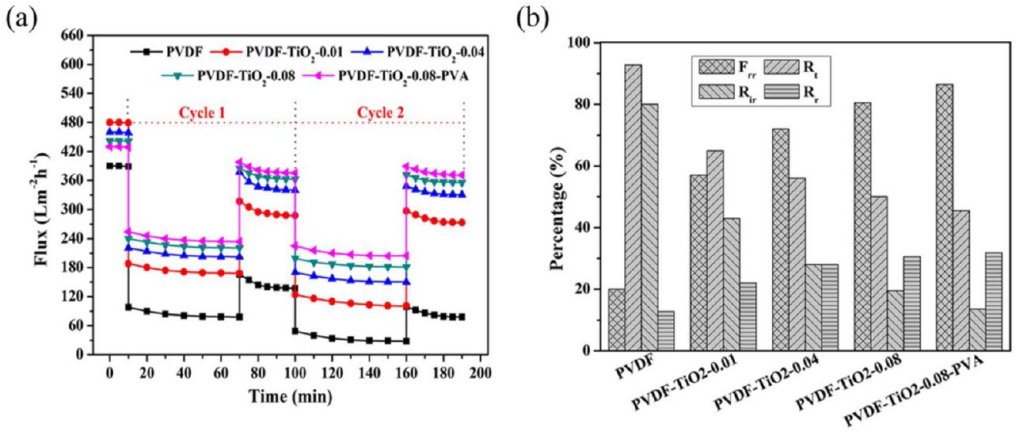

Figure 10. Evaluation the antifouling property of the pristine PVDF membrane and modified membranes: (a) time-dependent flux of pristine and modified membranes under two cycles of BSA solution filtration measurements; (b) comparison of R_t, R_r, R_{ir}, and F_{rr} of the pristine and modified membranes under two cycles of BSA solution filtration measurements.

linking of PVA, a pure water flux of PVDF/TiO_2-0.08/PVA is maintained at an appropriate value (430 L m^{-2} h^{-1}) compared with pristine membrane, while BSA rejection is significantly increased from 44.7% to 86.5%. This phenomenon can be interpreted from the fact that the cross-linked PVA layer would probably block part of the membrane pores, resulting in a great increase of BSA rejection. It is concluded that a higher BSA rejection can be obtained through TiO_2 nanoparticles and PVA modification, and an appropriate permeability for membrane filtration can still be maintained under an appropriate condition.

Antifouling Property of Membranes. In order to investigate the antifouling property of pristine and modified membranes, two cyclic filtration tests have been designed using BSA as a model protein. Each membrane used for characterizing the antifouling property has compacted at 0.1 MPa with deionized water for 40 min; then the transmembrane pressure was kept at 0.1 MPa through the whole filtration process. As shown in Figure 10a, the BSA flux for all membranes experiences a dramatic decrease due to the deposition and adsorption of BSA on the surface of membranes, and PVDF/TiO_2-0.08/PVA presents a maximum BSA flux (204 L m^{-2} h^{-1}) among the membranes. After a simple physical cleaning by deionized water, the water flux of all membranes could not recover completely because the BSA molecules may be entrapped in the pores. It is obvious that the recovery water flux of all modified membranes is higher than that of pristine membrane under same operating conditions due to the improvement of antifouling property. Additionally, it can be found that the water permeability of pristine membrane is gradually decreased during the operation process, while it is maintained at an appropriate value after one cycle of filtration measurement for modified membranes.

To quantitatively investigate the antifouling property during foulant filtration in detail, a summary of R_t, R_r, R_{ir}, and F_{rr} of the investigated membranes is shown in Figure 10b. It is obvious that R_t and R_{ir} for pristine membrane achieve 92.8% and 80%, respectively. However, a decreased R_t and R_{ir} could be observed for the PVDF/TiO_2/PVA modification membrane. It clearly demonstrates that the antifouling property has been effectively improved through TiO_2 and PVA surface modification. Additionally, it can be found that the tendency in R_{ir} is consistent with that of water contact angle, because membrane fouling should be directly correlated to the hydrophilicity of the membrane surface.[53,54] More TiO_2 nanoparticles bonded on the membrane surface with increasing TiO_2 concentration will induce the formation of a dense and stable hydration layer on the membrane surface, which will increase the BSA fouling resistance and reduce membrane fouling to some extent.[55] As a result, R_{ir} of PVDF/TiO_2 membrane decreases with increasing TiO_2 concentration. The F_{rr} of pristine membrane and PVDF/TiO_2-0.08 membrane after two cycles of filtration measurements is 20% and 80.5%, respectively, suggesting that TiO_2 modification indeed effectively decreases the deposition and adsorption of protein on the membrane surface. This can be further proved by the surface morphology of pristine and modified membranes as shown in Figure 11. It can be clearly found that amounts of BSA are accumulated on the pristine membrane surface, while no BSA could be found on a modified membrane surface. In addition, F_{rr} is continuously increased from 80.5% for PVDF/TiO_2-0.08 to 86.4% for PVDF/TiO_2-0.08/PVA due to adsorption-cross-linking of PVA on the membrane and TiO_2 nanoparticles surface. The above result demonstrates that the antifouling property of modified membranes is significantly improved by the perfect binding of TiO_2 nanoparticles on the PVDF membrane surface.

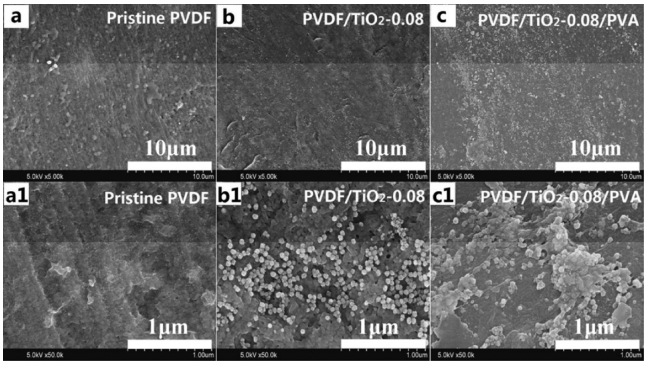

Figure 11. Surface morphology of pristine PVDF membrane (a), PVDF/TiO_2-0.08 membrane (b), and PVDF/TiO_2-0.08/PVA membrane (c) after two cycles of BSA solution filtration measurements; (a1, b1, and c1) partial enlarged views of pristine PVDF membrane (a), PVDF/TiO_2-0.08 membrane (b), and PVDF/TiO_2-0.08/PVA membrane (c), respectively.

DOI: 10.1021/acsami.5b00978
ACS Appl. Mater. Interfaces 2015, 7, 8427−8436

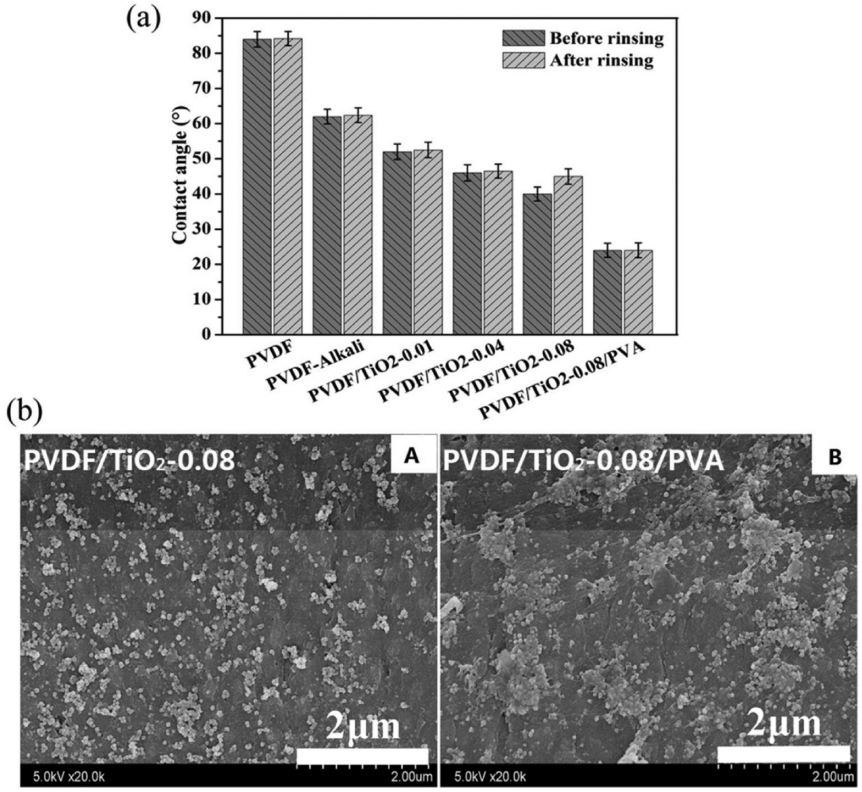

Figure 12. Evaluation of the binding performance of PVA layer and TiO_2 nanoparticles on membrane surface: (a) water contact angle of the various membranes before and after distilled water rinsing test; (b) surface morphology of PVDF/TiO_2-0.08 membrane (A) and PVDF/TiO_2-0.08/PVA membrane (B) after rinsing test (rinsing test was carried out with distilled water at 1000 r/min for 2 h).

Binding Performance of PVA Layer and TiO_2 Nanoparticles. Water contact angle measurements were carried out to verify the binding performance of TiO_2 and PVA layer. As shown in Figure 12a, the contact angle for PVDF/TiO_2-0.01 and PVDF/TiO_2-0.04 keeps constant before and after distilled water rinsing test, which indicates the good binding between TiO_2 nanoparticles and the membrane surface under a low TiO_2 concentration. Nevertheless, the contact angle of PVDF/TiO_2-0.08 is increased by 4° after rinsing. This phenomenon should be ascribed to the generation of some small TiO_2 clusters under a relatively high TiO_2 concentration, which can be probably washed away from the membrane surface in the rinsing process due to the weak interaction. However, the water contact angle of PVDF/TiO_2-0.08/PVA is far below that of PVDF/TiO_2-0.08 and keeps constant after the rinsing process. This reflects that the adsorption-cross-linking of PVA can further enhance the hydrophilicity of the membrane surface and effectively fix the separate TiO_2 nanoparticles on the membrane surface. Thereby, it can be concluded that TiO_2 nanoparticles can be firmly bonded on the membrane surface via the combination of chemical bonding and adsorption-cross-linking of PVA. On the other hand, the membrane surface morphology before and after rinsing in Figure 12b shows that there is almost no morphology change for the modified membrane surface after rinsing. This also demonstrates the fixed action of TiO_2 nanoparticles for the PVA layer, which effectively inhibits the peeling or delamination between the PVA layer and the membrane surface during the long-term operation process.

CONCLUSIONS

A novel hydrophilic PVDF ultrafiltration membrane was fabricated via a facile and versatile strategy to perfectly bind TiO_2 nanoparticles and a PVA layer onto a PVDF membrane surface simultaneously. TiO_2 nanoparticles were tightly bound onto the membrane surface through the combination of chemical bonding and adsorption-cross-linking of PVA, implying the remarkable binding ability of the surface-tailored TiO_2 nanoparticles. Meanwhile, the bonded TiO_2 nanoparticles provided some anchor sites for the PVA layer, which effectively inhibited the peeling or delamination of the PVA layer from the membrane surface. This modification process significantly improved the wettability of membranes and converted the membrane surface from hydrophobic to hydrophilic. A significant enhancement of antifouling property was further observed due to formation of a hydration layer on the membrane surface. This binding method not only provided a strong binding force but also kept membrane performance, suggesting great potential for binding nanoparticles to substrate surface.

AUTHOR INFORMATION

Corresponding Author

*Tel.: 86-21-67792842. Fax: 86-21-67792855. E-mail: chunjuhe@dhu.edu.cn.

Notes

The authors declare no competing financial interest.

ACKNOWLEDGMENTS

This work was supported by grants from the National High-tech Research and Development Projects

DOI: 10.1021/acsami.5b00978
ACS Appl. Mater. Interfaces 2015, 7, 8427−8436

(863,2012AA03A605), Program for New Century excellent talents (NCET-12-0827), Natural Science Foundation of China (Nos. 51103019 and 21174027), Program of Introducing Talents of Discipline to Universities (No.111-2-04), and Chinese Universities Scientific Fund (DH-D-2013017).

REFERENCES

(1) Kang, G.-D.; Cao, Y.-M. Application and Modification of Poly(vinylidene fluoride) (PVDF) Membranes—A review. *J. Membr. Sci.* **2014**, *463*, 145−165.
(2) Liu, F.; Hashim, N. A.; Liu, Y.; Abed, M. R. M.; Li, K. Progress in the Production and Modification of PVDF Membranes. *J. Membr. Sci.* **2011**, *375*, 1−27.
(3) Sun, A. C.; Kosar, W.; Zhang, Y.-F.; Feng, X.-S. A Study of Thermodynamics and Kinetics Pertinent to Formation of PVDF Membranes by Phase Inversion. *Desalination* **2013**, *309*, 156−164.
(4) Zhao, X.-T.; Su, Y.-L.; Li, Y.-F.; Zhang, R.-N.; Zhao, J.-J.; Jiang, Z.-Y. Engineering Amphiphilic Membrane Surfaces Based on PEO and PDMS Segments for Improved Antifouling Performances. *J. Membr. Sci.* **2014**, *450*, 111−123.
(5) Liang, S.; Qi, G.-G.; Xiao, K.; Sun, J.-Y.; Giannelis, E. P.; Huang, X.; Elimelech, M. Organic Fouling Behavior of Superhydrophilic Polyvinylidene Fluoride (PVDF) Ultrafiltration Membranes Functionalized with Surface-tailored Nanoparticles: Implications for Organic Fouling in Membrane Bioreactors. *J. Membr. Sci.* **2014**, *463*, 94−101.
(6) Zhang, F.; Zhang, W.-B.; Yu, Y.; Deng, B.; Li, J.-Y.; Jin, J. Sol−Gel Preparation of PAA-g-PVDF/TiO_2 Nanocomposite Hollow Fiber Membranes with Extremely High Water Flux and Improved Antifouling Property. *J. Membr. Sci.* **2013**, *432*, 25−32.
(7) Sui, Y.; Wang, Z.-N; Gao, C.-J; Wan, Q.; Zhu, L.-P. An Investigation on the Antifouling Ability of PVDF Membranes by Poly-DOPA Coating. *Desalin. Water Treat.* **2012**, *50*, 22−33.
(8) Guillen-Burrieza, E.; Ruiz-Aguirre, A.; Zaragoza, G.; Arafat, H. A. Membrane Fouling and Cleaning in Long Term Plant-scale Membrane Distillation Operations. *J. Membr. Sci.* **2014**, *468*, 360−372.
(9) Lee, J.-W.; Jung, J.-Y.; Cho, Y.-H.; Yadav, S.-K.; Baek, K.-Y.; Park, H.-B.; Hong, S.-M.; Koo, C.-M. Fouling-Tolerant Nanofibrous Polymer Membranes for Water Treatment. *ACS Appl. Mater. Interfaces* **2014**, *6*, 14600−14607.
(10) Park, S.-Y.; Chung, J.-W.; Chae, Y.-K.; Kwak, S.-Y. Amphiphilic Thiol Functional Linker Mediated Sustainable Anti-Biofouling Ultrafiltration Nanocomposite Comprising a Silver Nanoparticles and Poly(vinylidene fluoride) Membrane. *ACS Appl. Mater. Interfaces* **2013**, *5*, 10705−10714.
(11) Li, X.-F.; Zhou, C.; Du, R.-H.; Li, N.-N.; Han, X.-T.; Zhang, Y.-F.; An, S.-L.; Xiao, C.-F. Evolution of Polyvinylidene Fluoride (PVDF) Hierarchical Morphology during Slow Gelation Process and Its Superhydrophobicity. *ACS Appl. Mater. Interfaces* **2013**, *5*, 5430−5435.
(12) Mansouri, J.; Harrisson, S.; Chen, V. Strategies for Controlling Biofouling in Membrane Filtration Systems: Challenges and Opportunities. *J. Mater. Chem.* **2010**, *20*, 4567−4586.
(13) Zuo, G.-Z.; Wang, R. Novel Membrane Surface Modification to Enhance Anti-oil Fouling Property for Membrane Distillation Application. *J. Membr. Sci.* **2013**, *447*, 26−35.
(14) Ben-Sasson, M.; Zodrow, K. R.; Genggeng, Q.; Kang, Y.; Giannelis, E. P.; Elimelech, M. Surface Functionalization of Thin-Film Composite Membranes with Copper Nanoparticles for Antimicrobial Surface Properties. *Environ. Sci. Technol.* **2013**, *48*, 384−393.
(15) Zhou, R.; Ren, P.-F.; Yang, H.-C.; Xu, Z.-K. Fabrication of Antifouling Membrane Surface by Poly(sulfobetaine methacrylate)/Polydopamine Co-Deposition. *J. Membr. Sci.* **2014**, *466*, 18−25.
(16) Nishigochi, S.; Ishigami, T.; Maruyama, T.; Hao, Y.; Ohmukai, Y.; Iwasaki, Y.; Matsuyama, H. Improvement of Antifouling Properties of Polyvinylidene Fluoride Hollow Fiber Membranes by Simple Dip Coating of Phosphorylcholine Copolymer via Hydrophobic Interactions. *Ind. Eng. Chem. Res.* **2014**, *53*, 2491−2497.
(17) Meng, S.-W.; Mansouri, J.; Ye, Y.; Chen, V. Effect of Templating Agents on the Properties and Membrane Distillation Performance of TiO_2-Coated PVDF Membranes. *J. Membr. Sci.* **2014**, *450*, 48−59.
(18) Razmjou, A.; Arifin, E.; Dong, G.-X.; Mansouri, J.; Chen, V. Superhydrophobic Modification of TiO_2 Nanocomposite PVDF Membranes for Applications in Membrane Distillation. *J. Membr. Sci.* **2012**, *415−416*, 850−863.
(19) Oh, S.-J.; Kim, N.-W.; Lee, Y.-T. Preparation and Characterization of PVDF/TiO_2 Organic−Inorganic Composite Membranes for Fouling Resistance Improvement. *J. Membr. Sci.* **2009**, *345*, 13−20.
(20) Yu, L.-Y.; Xu, Z.-L.; Shen, H.-M.; Yang, H. Preparation and Characterization of PVDF−SiO_2 Composite Hollow Fiber UF Membrane by Sol−Gel Method. *J. Membr. Sci.* **2009**, *337*, 257−265.
(21) Liang, S.; Kang, Y.; Tiraferri, A.; Giannelis, E. P.; Huang, X.; Elimelech, M. Highly Hydrophilic Polyvinylidene Fluoride (PVDF) Ultrafiltration Membranes via Postfabrication Grafting of Surface-Tailored Silica Nanoparticles. *ACS Appl. Mater. Interfaces* **2013**, *5*, 6694−6703.
(22) Yan, L.; Li, Y.-S.; Xiang, C.-B. Preparation of Poly(vinylidene fluoride)(pvdf) Ultrafiltration Membrane Modified by Nano-Sized Alumina (Al_2O_3) and its Antifouling Research. *Polymer* **2005**, *46*, 7701−7706.
(23) Zhao, X.-Y.; Ma, J.; Wang, Z.-H.; Wen, G.; Jiang, J.; Shi, F.-M.; Sheng, L.-X. Hyperbranched-polymer Functionalized Multi-walled Carbon Nanotubes for Poly (vinylidene fluoride) Membranes: From Dispersion to Blended Fouling-control Membrane. *Desalination* **2012**, *303*, 29−38.
(24) Ma, J.-L.; Zhao, Y.-F.; Xu, Z.-W.; Min, C.-Y.; Zhou, B.-M.; Li, Y.-L.; Li, B.-D.; Niu, J.-R. Role of Oxygen-containing Groups on MWCNTs in Enhanced Separation and Permeability Performance for PVDF Hybrid Ultrafiltration Membranes. *Desalination* **2013**, *320*, 1−9.
(25) Wang, Q.-Q.; Wang, X.-T.; Wang, Z.-H.; Huang, J.; Wang, Y. PVDF Membranes with Simultaneously Enhanced Permeability and Selectivity by Breaking the Tradeoff Effect via Atomic Layer Deposition of TiO_2. *J. Membr. Sci.* **2013**, *442*, 57−64.
(26) Song, H.-C.; Shao, J.-H.; He, Y.-L.; Liu, B.; Zhong, X.-Q. Natural Organic Matter Removal and Flux Decline with PEG−TiO_2-Doped PVDF Membranes by Integration of Ultrafiltration with Photocatalysis. *J. Membr. Sci.* **2012**, *405−406*, 48−56.
(27) Rana, D.; Matsuura, T. Surface Modifications for Antifouling Membranes. *Chem. Rev.* **2010**, *110*, 2448−2471.
(28) Li, J.-H.; Xu, Y.-Y.; Zhu, L.-P.; Wang, J.-H.; Du, C.-H. Fabrication and Characterization of a Novel TiO_2 Nanoparticle Self-Assembly Membrane with Improved Fouling Resistance. *J. Membr. Sci.* **2009**, *326*, 659−666.
(29) Bae, T.-H.; Kim, I.-C.; Tak, T.-M. Preparation and Characterization of Fouling-Resistant TiO_2 Self-Assembled Nanocomposite Membranes. *J. Membr. Sci.* **2006**, *275*, 1−5.
(30) Luo, M.-L.; Zhao, J.-Q.; Tang, W.; Pu, C.-S. Hydrophilic Modification of Poly(ether sulfone) Ultrafiltration Membrane Surface by Self-Assembly of TiO_2 Nanoparticles. *Appl. Surf. Sci.* **2005**, *249*, 76−84.
(31) Bae, T.; Tak, T. Preparation of TiO_2 Self-Assembled Polymeric Nanocomposite Membranes and Examination of Their Fouling Mitigation Effects in a Membrane Bioreactor System. *J. Membr. Sci.* **2005**, *266*, 1−5.
(32) M'barki, O.; Hanafia, A.; Bouyer, D.; Faur, C.; Sescousse, R.; Delabre, U.; Blot, C.; Guenoun, P.; Deratani, A.; Quemener, D.; Pochat-Bohatier, C. Greener Method to Prepare Porous Polymer Membranes by Combining Thermally Induced Phase Separation and Crosslinking of Poly(vinyl alcohol) in Water. *J. Membr. Sci.* **2014**, *458*, 225−235.
(33) Kozlov, M.; Quarmyne, M.; Chen, W.; McCarthy, T. J. Adsorption of Poly(vinyl alcohol) onto Hydrophobic Substrates. A General Approach for Hydrophilizing and Chemically Activating Surfaces. *Macromolecules* **2003**, *36*, 6054−6059.
(34) Li, N.-N.; Xiao, C.-F.; An, S.-L.; Hu, X.-Y. Preparation and Properties of PVDF/PVA Hollow Fiber Membranes. *Desalination* **2010**, *250*, 530−537.

DOI: 10.1021/acsami.5b00978
ACS Appl. Mater. Interfaces 2015, 7, 8427−8436

(35) Guo, R.-L.; Fang, X.; Wu, H.; Jiang, Z.-Y. Preparation and Pervaporation Performance of Surface Cross-linked PVA/PES Composite Membrane. *J. Membr. Sci.* **2008**, *322*, 32−38.
(36) Zhang, J.; Wang, Q.-Y.; Wang, Z.-W.; Zhu, C.-W.; Wu, Z.-C. Modification of Poly(vinylidene fluoride)/Polyethersulfone Blend Membrane with Polyvinyl Alcohol for Improving Antifouling Ability. *J. Membr. Sci.* **2014**, *466*, 293−301.
(37) Hao, J.-W.; Wu, Y.-H.; Ran, J.; Wu, B.; Xu, T.-W. A Simple and Green Preparation of PVA-based Cation Exchange Hybrid Membranes for Alkali Recovery. *J. Membr. Sci.* **2013**, *433*, 10−16.
(38) Du, J. R.; Peldszus, S.; Huck, P. M.; Feng, X.-S. Modification of Poly(vinylidene fluoride) Ultrafiltration Membranes with Poly(vinyl alcohol) for Fouling Control in Drinking Water Treatment. *Water Res.* **2009**, *43*, 4559−4568.
(39) Puspitasari, V.; Granville, A.; Le-Clech, P.; Chen, V. Cleaning and Ageing Effect of Sodium Hypochlorite on Polyvinylidene Fluoride (PVDF) Membrane. *Sep. Purif. Technol.* **2010**, *72*, 301−308.
(40) Brewis, D. M.; Mathieson, I.; Sutherland, I.; Cayless, R. A.; Dahm, R. H. Pretreatment of Poly(vinyl fluoride) and Poly(vinylidene fluoride) with Potassium Hydroxide. *Int. J. Adhes. Adhes.* **1996**, *16*, 87−95.
(41) Ross, G. J.; Watts, J. F.; Hill, M. P.; Morrissey, P. Surface Modification of Poly(vinylidene fluoride) by Alkaline Treatment1. The Degradation Mechanism. *Polymer* **2000**, *41*, 1685−1696.
(42) Martins, P.; Lopes, A. C.; Lanceros-Mendez, S. Electroactive Phases of Poly(vinylidene fluoride): Determination, Processing and Applications. *Prog. Polym. Sci.* **2014**, *39*, 683−706.
(43) Boccaccio, T.; Bottino, A.; Capannelli, G.; Piaggio, P. Characterization of PVDF Membranes by Vibrational Spectroscopy. *J. Membr. Sci.* **2002**, *210*, 315−329.
(44) Ross, G. J.; Watts, J. F.; Hill, M. P.; Morrissey, P. Surface Modification of Poly(vinylidene fluoride) by Alkaline Treatment Part 2. Process Modification by the Use of Phase Transfer Catalysts. *Polymer* **2001**, *42*, 403−413.
(45) Chen, N.-P.; Hong, L. Surface Phase Morphology and Composition of the Casting Films of PVDF−PVP Blend. *Polymer* **2002**, *43*, 1429−1436.
(46) Zhao, C.-Q.; Xu, X.-C.; Chen, J.; Wang, G.-W.; Yang, F.-L. Highly Effective Antifouling Performance of PVDF/Graphene Oxide Composite Membrane in Membrane Bioreactor (MBR) System. *Desalination* **2014**, *340*, 59−66.
(47) Wang, P.-P.; Ma, J.; Wang, Z.-H.; Shi, F.-M.; Liu, Q.-L. Enhanced Separation Performance of PVDF/PVP-g-MMT Nanocomposite Ultrafiltration Membrane Based on the NVP-Grafted Polymerization Modification of Montmorillonite (MMT). *Langmuir* **2012**, *28*, 4776−4786.
(48) Chang, X.-J.; Wang, Z.-X.; Quan, S.; Xu, Y.-C.; Jiang, Z.-X.; Shao, L. Exploring the Synergetic Effects of Graphene Oxide (GO) and Polyvinylpyrrodione (PVP) on Poly(vinylylidenefluoride) (PVDF) Ultrafiltration Membrane Performance. *Appl. Surf. Sci.* **2014**, *316*, 537−548.
(49) Wang, M.-C.; Fang, D.-W.; Wang, N.-N.; Jiang, S.; Nie, J.; Yu, Q.; Ma, G.-P. Preparation of PVDF/PVP Core−Shell Nanofibers Mats via Homogeneous Electrospinning. *Polymer* **2014**, *55*, 2188−2196.
(50) Zhang, P.; Shao, C.-L.; Zhang, Z.-Y.; Zhang, M.-Y.; Mu, J.-B.; Guo, Z.-C.; Liu, Y.-C. TiO_2@Carbon Core/Shell Nanofibers: Controllable Preparation and Enhanced Visible Photocatalytic Properties. *Nanoscale* **2011**, *3*, 2943.
(51) Wang, D.-S.; Xiao, L.-B.; Luo, Q.-Z.; Li, X.-Y.; An, J.; Duan, Y.-D. Highly Efficient Visible Light TiO_2 Photocatalyst Prepared by Sol−Gel Method at Temperatures Lower Than 300°C. *J. Hazard. Mater.* **2011**, *192*, 150−159.
(52) Lang, W.-Z.; Zhang, X.; Shen, J.-P.; Xu, H.-P.; Xu, Z.-L.; Guo, Y.-J. The Contrastive Study of Chemical Treatment on the Properties of PVDF/PFSA and PVDF/PVP Ultrafiltration Membranes. *Desalination* **2014**, *341*, 72−82.
(53) Sigal, G. B.; Mrksich, M.; Whitesides, G. M. Effect of Surface Wettability on the Adsorption of Proteins and Detergents. *J. Am. Chem. Soc.* **1998**, *120*, 3464−3473.
(54) van der Marel, P.; Zwijnenburg, A.; Kemperman, A.; Wessling, M.; Temmink, H.; van der Meer, W. Influence of Membrane Properties on Fouling in Submerged Membrane Bioreactors. *J. Membr. Sci.* **2010**, *348*, 66−74.
(55) Peng, J.-M.; Su, Y.-L.; Shi, Q.; Chen, W.-J.; Jiang, Z.-Y. Protein Fouling Resistant Membrane Prepared by Amphiphilic Pegylated Polyethersulfone. *Bioresour. Technol.* **2011**, *102*, 2289−2295.

DOI: 10.1021/acsami.5b00978
ACS Appl. Mater. Interfaces 2015, 7, 8427−8436